Effect of Molecular Architecture on the Adsorption of Copolymers

Anna C. Balazs* and Michael Gempe

Materials Science and Engineering Department, University of Pittsburgh, Pittsburgh, Pennsylvania 15261

Christopher W. Lantman

Mobay Corporation, Bayer USA Inc., Pittsburgh, Pennsylvania 15205-9741

Received April 19, 1990; Revised Manuscript Received June 18, 1990

ABSTRACT: We developed Monte Carlo computer simulations to model the adsorption of AB copolymers from solution onto a solid surface. Using this model, we examined the role that the arrangement of the monomers in the copolymer plays in determining the structure of the adsorbed film. The comonomer sequence is varied from alternating to random to various blocky arrangements. We assume that the A comonomer is attracted to the surface, while the B monomer is unreactive with, or repelled by, the interface. We find that the structure of the adlayer is sensitive not only to the amount of A present in the chain but also to the arrangement of the A units along the chain. These findings are relevant to such applications as steric stabilization, adhesion, and lubrication.

Introduction

The adsorption and structure of polymers at interfaces is an area of current scientific interest. In addition to homopolymer studies,[1] the surface adsorption of diblocks,[2] triblocks,[3-6] and, most recently, random copolymers[5,7-9] has been investigated. Furthermore, a variety of surface topologies have been examined, from flat to rough[10-12] and impenetrable to penetrable.[7,8,13] By comparison of the findings of these investigations, it is clear that the structure of the adlayer is sensitive to the architecture of the polymer chain. In this paper, we present a series of studies aimed at clarifying the role that the arrangement of the monomers in the copolymer plays in determining the equilibrium structure of the adsorbed film. The comonomer sequence is varied from alternating to random to blocky. We examine the situation where one comonomer tends to adsorb but the second comonomer is unreactive with, or repelled by, the interface. Adsorption under each of these conditions is studied on a flat, impenetrable surface. In a subsequent paper, we will describe the behavior of a range of multiblock copolymers at the penetrable interface between two immiscible fluids,[14] the so-called "phantom" wall.[7] The results from such studies will ultimately indicate how to tailor the polymer geometry to provide the optimal conditions for such applications as steric stabilization, enhanced adhesion, and wettability.

To undertake this study, we developed Monte Carlo computer simulations to model the adsorption of various chains from solution onto a surface. In this model, we assume that the binding between the polymers and the surface is reversible. Consequently, the chains can undergo structural rearrangements in response to energetic or entropic constraints at the surface. We note that both thermodynamic and kinetic forces play a role in the simulation. The thermodynamic driving force for polymer adsorption is generally thought to be solvent incompatibility, yet this driving force will clearly be mediated by kinetic effects that hinder the transport of polymer to the surface. The balance between these thermodynamic and kinetic effects should govern the adsorption process and resulting structure of the adsorbed layer.

In an attempt to elucidate the effect of chain geometry, computer simulations pose significant advantages over other techniques. First, chemically precise and identical chains can be created in the simulation. This allows us to precisely and independently vary such factors as sequence distribution, molecular weight, and molecular weight distribution, interaction energy, and solution concentration. While analytical models may also allow for the specification of these parameters, determining the influence of sequence distribution on adsorption through such methods has proven to be difficult.[7] Second, the simulations provide a view of the microscopic behavior not only at the surface but also in the subsequent layers of the polymer film. Thus, we can calculate the total segment density distribution normal to the interface, as well as the amount of polymer bound directly on the surface. These calculations can be made separately for each comonomer.

In this report, we will contrast the surface adsorption from solutions containing random, alternating, or blocky AB copolymers. The A monomers are strongly attracted to the surface, while the B molecules are not. We also consider the case where the B sites are in fact repelled from this wall. By calculating the surface coverage and density profiles obtained from each type of solution, we can determine the effect of sequence distribution on polymer–surface interactions. Below, we describe the model we used to examine the interfacial properties of such chains. We then describe our results for the adsorption of AB copolymers onto solid surfaces.

The Model

We start by describing the simulation for polymer adsorption onto a solid, impenetrable wall. The wall is the $Z = 0$ plane in a cubic box that is $50 \times 50 \times 50$ lattice sites in size. Twenty self-avoiding random-walk chains are placed at random locations in this cube. The chains are allowed to diffuse throughout this volume. The diffusive motion consists of "wiggling" the chain via the Verdier and Stockmayer[15] and Hilhorst and Deutch[16] algorithm for chain dynamics and then translating the entire chain one lattice site in one of the six possible directions (to be chosen at random). All attempted moves obey the excluded-volume criteria. If a chain diffuses out of the confines of the above cube, it is "killed" and a new chain is introduced at a random location in this volume.

Next, one of the chains in the system is chosen at random and one of the beads on this chain is randomly selected. The chain is wiggled about this bead and translated. These

0024-9297/91/2224-0168$02.50/0 © 1991 American Chemical Society

free chains continue to diffuse until an A site (or "sticker") is one lattice unit above a surface site. Then the A bead remains bound at this location, while the remainder of the chain is free to wiggle about this point of attachment. Whenever any subsequent A bead is one lattice site above the surface, it binds at that location, thus modeling the strong affinity between an A monomer and the surface. The intervening B units are still allowed to wiggle about the points of attachment (under the constraint that the chain does not break at any time). Thus, even if a B segment now comes in contact with a surface site, in a later move, it can wiggle away from its surface location. This aspect of the program models the weak B–surface interaction and strong B–solvent affinity.

Whenever a free chain becomes bound to the surface, a new chain is added at a random location in the solution above the wall. Thus, the number of chains in the solution remains constant throughout the simulation.

In this set of simulations, we assume that the binding between an A bead and the surface is reversible. Two different models for reversibility were utilized, and the results were subsequently compared to ensure that the modeling algorithms accurately depict reversible binding. In the first model, which we will refer to as the "segmental desorption" model, each A–surface contact is reversible. Specifically, when a bound chain is randomly selected from all the chains in the system and, furthermore, a bound A bead is picked from the units on the chain, the single A sticker is allowed to wiggle off the surface with a specified probability, P. Here, we have set P equal to 1.0 in order to produce an appreciable degree of desorption. Only a single A bead is allowed to desorb per unit time step: if the wiggling motion also causes contiguous A sites to desorb, the move is rejected. If B sites, on the other hand, are simultaneously desorbed in the course of the wiggle, the move is accepted. These rules model the fact that the chain is tethered to the surface through the strong A–surface bonds. Application of these rules means that if an A bead is collinear with other adsorbed A's on both its sides, the bead cannot desorb. Thus, the end of an A block must desorb before any subsequent A beads can leave the surface. Once an A end has been freed, subsequent A's can "flip" to a new position off the wall. In effect, a run of A's must "peel" off, starting from an end site, in order for the segment to be freed from the surface. (This "peeling" action can be initiated from either end of the run of A's).

When a particular A bead desorbs, it may wiggle back to a surface position in a subsequent move and, thus, once again become bound.

When a chain desorbs (all the beads are now at least two lattice sites above the surface), it is translated in a direction to be picked at random: either in the four directions parallel to the interface, or one lattice site vertically up, or one lattice site vertically down. In the latter case, the chain again becomes bound to the surface. If, one the other hand, the chain remains free, the chain furthest from the $Z = 0$ wall is removed from the box. This ensures that the number of free chains in solution remains constant at 20.

Initially, the chains can desorb without significant hindrance from other adsorbed chains. As the surface becomes more crowded, steric hindrance from neighboring chains will make this desorption more and more difficult.

In the second method, the "molecular desorption" model, a bound chain can break away from the surface with a prescribed probability P, which in turn is weighted by the number of A units in the chain that are bound to the surface. Thus, the total probability that a chain will desorb is given by

$$P_t = P^*(1/n) \tag{1}$$

where n is the number of bound A sites. (In these calculations, we have set P equal to 1.0 for all the cases considered below; this will ensure a sufficiently high frequency of desorption.) Thus, the chain–surface interaction has a finite lifetime, τ, which is inversely proportional to P_t.[17] In other words, the lifetime of a conformation is directly weighted by the number of A–surface contacts: the more A–surface contacts, the longer the chain remains at the surface.

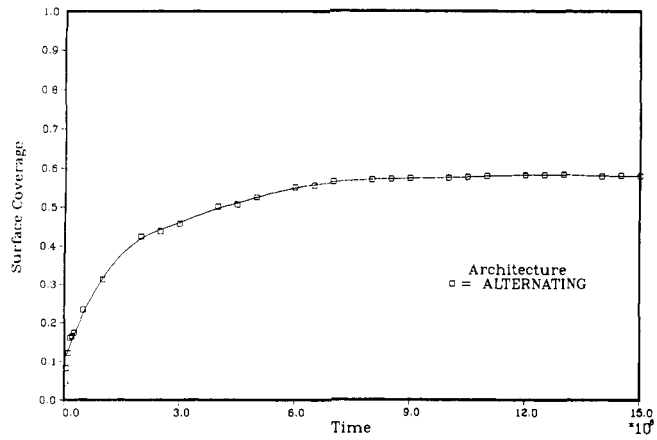

Figure 1. Plot of surface coverage versus time for the alternating $A_{17}B_{16}$ copolymers.

To implement the model, a random number generator is invoked: if the value produced by the generator is less than P_t, the polymer chain is considered to be a free chain. Next, a bead is picked at random and wiggled (according to the rules in refs 15 and 16). After the wiggle, the chain is translated in one of the six possible directions. These motions can cause the chain to become bound to the surface through totally different A beads than those that had tethered it to the interface in the previous configuration. To summarize, in a given time step, a bound chain is designated a free chain with a probability equal to P_t; it is then wiggled and translated, which can cause the chain to become reattached through different A stickers. Through this mechanism, the "molecular desorption" model also allows individual segments to desorb per unit time.

Here too, if a chain becomes free, the chain furthest from the $Z = 0$ surface is removed from the box. Again, as the surface becomes more crowded, adsorbed chains sterically hinder the desorbing chains from leaving the surface.

The simulations were run for 10–15 million time steps, that is, until the surface has effectively become saturated and the surface coverage reaches a plateau value. (Specifically, we run the simulation until three consecutive values, measured at 1 million time step intervals, *all* differ by less than 1%.) This stage is clearly visible in Figure 1, where we have plotted surface coverage versus time for a typical run. The values in the subsequent tables, which characterize the surface properties of the copolymers, are taken from this plateau region.

To model the scenario where the B–surface interaction is actually repulsive, we implement a modified version of the above simulation. Here, we again check to see if an A bead is on top of the surface site; however, now the probability that the chain will stick is weighted by the factor $q = \exp(-n_B\chi_{BS})$, where n_B is the number of B segments also in contact with the surface and χ_{BS} is the interaction energy between the surface and a B site.[18] The

Table I

polymer	f_A,[a] %	f_B,[b] %	no. of bound chains	surface coverage,[c] %	ave layer thickness[d]
			(a)		
alternating	40.2 ± 0.1	34.3 ± 0.2	115.5 ± 3.5	59.1 ± 2.0	5.41 ± 0.05
random	43.0 ± 1.4	29.2 ± 0.7	112.5 ± 2.1	56.3 ± 2.5	5.54 ± 0.09
blocky	53.2 ± 0.4	23.0 ± 2.2	97 ± 1.4	54.9 ± 0.3	5.16 ± 0.02
diblock	68.8 ± 2.9	5.15 ± 1.0	99.5 ± 1.4	52.2 ± 0.6	6.93 ± 0.06
triblock	73.5 ± 1.2	12.9 ± 1.5	88.5 ± 3.5	53.7 ± 2.4	5.36 ± 0.18
			(b) Segmental Desorption		
alternating	39.6 ± 0.3	32.7 ± 0.3	119 ± 2.8	58.2 ± 0.1	5.64 ± 0.05
random	48.7 ± 3.2	31.4 ± 0.6	110 ± 0.0	60.3 ± 2.5	5.32 ± 0.06
diblock	66.7 ± 3.15	5.6 ± 0.4	105.5 ± 2.1	53.8 ± 1.6	7.06 ± 0.05
$A_3B_{44}A_3$	80.6 ± 0.6	7.2 ± 1.0	81.5 ± 3.5	27.2 ± 2.8	8.33 ± 0.04
			(c)		
alternating	35.4 ± 0.8	27.2 ± 1.4	111.5 ± 1.4	48.1 ± 1.5	5.81 ± 0.06
blocky	57.5 ± 0.8	12.8 ± 0.8	92 ± 4.2	47.0 ± 1.1	5.31 ± 0.14

[a] Percent of A molecules bound to the surface. [b] Percent of B molecules bound to the surface. [c] Percent of sites at $Z = 0$ covered by polymer sites (either A or B). [d] This quantity is the maximum Z coordinate for each bound chain, averaged over all the adsorbed chains.

value of χ_{BS} is chosen to be greater than zero to reflect a repulsive interaction between these species. Again, two independent simulations, of 10–15 million time steps each, were averaged.

In all these investigations, we are focusing our attention on the nature of the polymer–surface interaction. Thus, we neglect chain–chain interactions in the solution and between free and adsorbed chains. Such interactions can be neglected in the case of polymer adsorption from dilute solutions, where the probability of chain–chain contact is small. It is for this scenario that our simulations are most appropriate.

Comparison of the Models

Before discussing the results concerning the effect of polymer architecture on adsorption, we will compare the results of the molecular and segmental desorption models. Both models were used to examine the surface properties of three separate types of $A_{17}B_{16}$ copolymers, alternating, random, and diblock, and of $A_3B_{44}A_3$ triblock copolymers. Table I contains the results obtained from both the models for each of these chain architectures. (Tables Ia and IIIa contain these results from the molecular model, while Table Ib displays the corresponding findings from the segmental model.) As can be seen, the differences between these models for all the cases examined are negligible. The reason for the similarity between these results is 2-fold. First, when the surface becomes sufficiently crowded, the effects of steric hindrance dominate the behavior of the chains at the interface and the desorption of a significant number of A's through either method becomes prohibited. Second, if the chains contain long contiguous runs of A's, the probability of large sections peeling off or desorbing becomes sufficiently small that these chains are not expected to undergo significant structural changes once they become bound to the surface.

Since both models provide essentially the same results, we have chosen the molecular desorption model for the calculations described below. Thus, all reported data were obtained by using this model with P set equal to 1.0.

Results and Discussion

Alternating, Random and Block Copolymers. The adsorption of AB copolymers where the A segments bind strongly to the surface and the B segments are noninteractive is discussed first. In a later section, we will discuss the case where the B segments are repelled by the surface. In the adsorption of copolymers, it is important to separate the effects of composition from those of sequence distribution. We therefore start the discussion with copolymers of identical composition but very different sequence distributions. Namely, we contrast the adsorption behavior of alternating, random, and blocky AB copolymer chains. In all these calculations, the AB chains are 33 lattice sites long: 17 sites represent A monomers and 16 sites are B monomers. Within each simulation, every chain has the same sequence distribution; from simulation to simulation, the chains differ only in the distribution of the monomers along the chain. In particular, the average run or block lengths $\langle n_A \rangle$ and $\langle n_B \rangle$ of the A and B sites[19] are both equal to 1 for the alternating sequence distribution. In the case of the random distribution, $\langle n_A \rangle = 1.86$ and $\langle n_B \rangle = 1.75$, and for a blocky chain, we chose $\langle n_A \rangle$ to be 6 lattice sites and set $\langle n_B \rangle$ equal to 5. In the diblock structure, all the A's are located at one end and all the B's are located at the other; thus, $\langle n_A \rangle = 17$ and $\langle n_B \rangle = 16$. Finally, for the triblock, a run of 8 B's are located on either side of the central string of 17 A's. In a later section we will relax the constraint of constant composition and present the results for ABA and BAB triblocks that have varying ratios of A and B molecules.

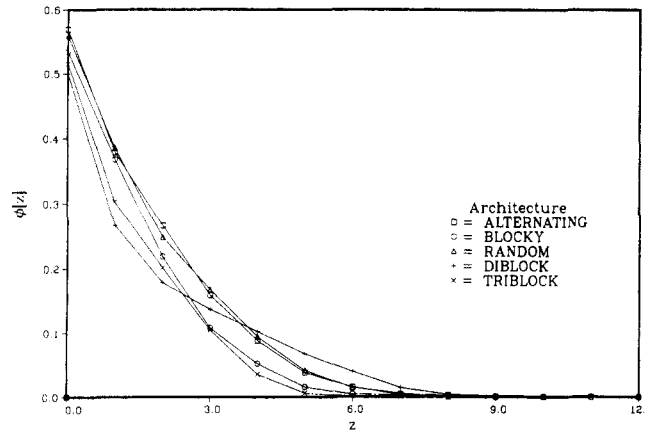

Figure 2. Segment density distributions (SSD's) normal to the wall for the alternating, random, and various blocky chains. The $\phi[z]$ values represent the total fraction of sites occupied by monomers A and B in the specified Z plane. All the chains in these simulations are 33 lattice sites long and contain 17 A's and 16 B's. Only the adsorbed chains are included in the calculation of the SDD. (Each plot represents values from a single run of the relevant simulation, while the values of surface coverage in the tables are obtained from averaging two independent simulation runs.)

Figure 2 shows the segment distribution density (SDD) normal to the wall for the alternating, random, blocky, and di- and triblock sequence distributions. Two distinctive

features can be observed from this graph. First, changes in comonomer sequence distribution yield subtle but real differences in the surface coverage (the amount of polymer, both A and B sites, directly on the $Z = 0$ layer) and the overall SDD. Second, the copolymers with shorter A block lengths yield higher surface coverages, while the diblock provides the greatest layer thickness. To understand these findings, further measurements were made; specifically, we calculated the fraction of A's and B's lying on the surface and the total number of chains bound to the wall.

Table Ia shows the fraction of A's and B's and total number of chains bound on the surface, as well as the surface coverage and layer thickness. The fraction of bound A's (B's) is defined as

$$n_i^b/Mn_i \tag{2}$$

where n_i^b is the number of A (B) segments in contact with the surface, M is the number of bound chains, and n_i is the number of i type (A or B) units in a given chain. The fraction of bound, sticky A's should provide a measure of the adhesion between the copolymer and the substrate. We observe that the fraction of bound A's is the *lowest* for the alternating case, which has the shortest run length. The fraction of bound A's is highest for the di- and triblock chains. These phenomena can be understood by viewing the graphical output from simulations for adsorption in two dimensions.

Figure 3a shows the conformation of a bound alternating copolymer in two dimensions. The dark circles represent bound A's, while the open circles represent the unbound A molecules. Since each sticker is separated by a B monomer, it is difficult to form long sections of contiguously bound species, or "trains", along the surface. Furthermore, whenever one sticker binds, it brings the entire chain within close proximity of the surface. Now, an A molecule at some distance from this bound unit, but close to the surface, can bind to the solid wall. This behavior further encourages the formation of loop or "hairpin" structures that extend away from the surface. The subsequent adsorption of new, incoming chains prevents already bound polymers from stretching out and thereby exposing more A's to the adsorbing wall. At high surface coverage, there is insufficient space for a significant fraction of the sticky A's; thus, a large number of the chains bind with long "tails" that stretch into the solution. All these factors contribute to the observation of a relatively low fraction of bound A molecules. On the other hand, the close proximity of the sticky A's to the nonreactive B's leads to the adsorption of several B monomers in the surface layer. Thus, the fraction of bound B's is relatively high for the alternating copolymer case. Finally, the narrow hairpins and long tails also account for a large layer thickness or extension in the Z direction (normal to the surface).

Figure 3c shows the graphical output for the blocky copolymer in two dimensions. As can be seen, the blocky copolymers have longer adsorbed A runs than their alternating analogues. The blocky chains initially adsorb in rows of stickers that stretch out along the surface. Here, the B's form short loops that lie away from the wall. Consequently, the fraction of B's in contact with this plane is lower for the blocky chain than the alternating copolymer. Furthermore, since the B molecules can only form small loops and the majority of the A's are bound to the surface, the resulting film is relatively thin compared to the other chain geometries (see Figure 2).

Figure 3d shows diblock copolymers bound to the surface in two dimensions. Since $\langle n_A \rangle$ is greater here than in the case of the blocky chain, longer trains of sticky A's lie along the surface. Consequently, the fraction of the bound A's is higher in this case than the previous two. The nonreactive B's all lie at one end of the chain, which is now free to extend into the compatible solvent in a taillike conformation. Since there are no additional A monomers at the end of these B tails, they are not energetically driven to return to the surface. Consequently, the fraction of bound B's is lowest for this conformation. At high surface coverage, not all the A's can be accommodated directly on the interface, thus some fraction of A's form small loops or constitute a part of the tails that extend into the solution (see Figure 3d). These long tails, whether they are purely B or contain a fraction of A's, are responsible for the largest layer thickness amongst all the structures examined. This analysis helps to explain the unique shape of the SDD curve

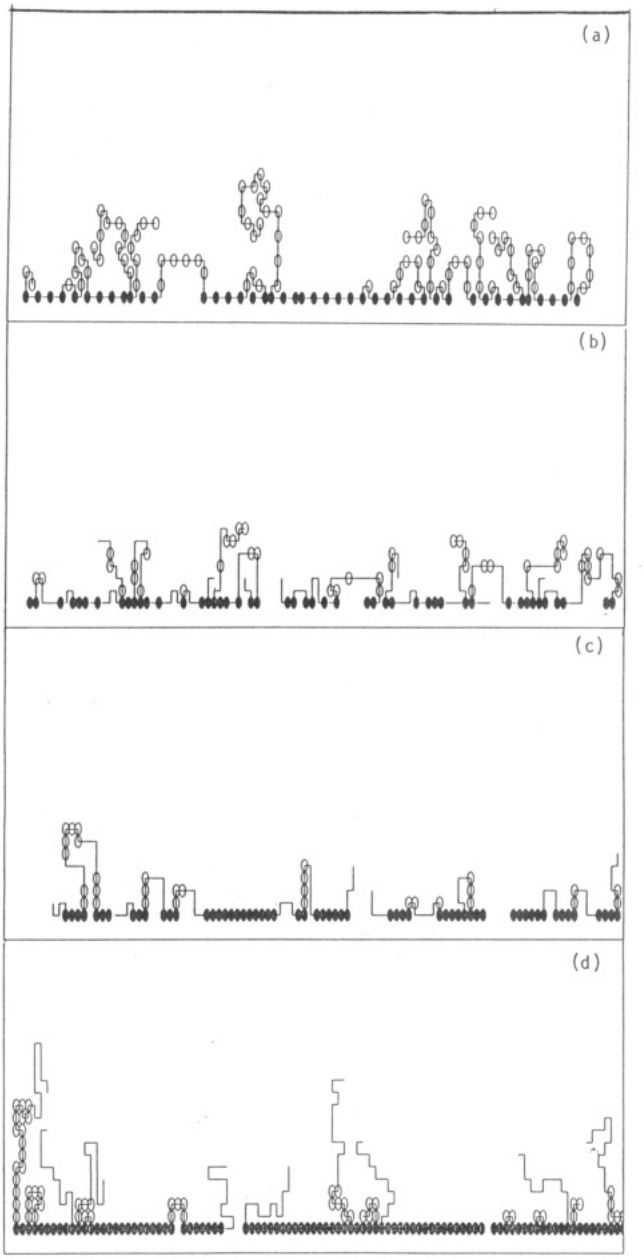

Figure 3. Graphical output from the simulations performed in two dimensions. Frame (a) shows the conformations of the bound alternating copolymers; (b) displays random copolymers adsorbed at the interface; (c) shows blocky copolymers that are attached to the wall; (d) depicts the structure of adsorbed diblocks. The dark circles represent bound A molecules, while the open circles depict the unbound A's. All the chains in these simulations are 33 lattice sites long and contain 17 A's and 16 B's.

for the diblock copolymer. Since the majority of the A's lie along the surface, there is a dearth of A's in a subsequent layer. Furthermore, there is only one B tail per chain, which, due to long run of bound A's, may be spaced far from another B block. Consequently, there are few molecules located in the layers above the surface. In fact, the polymer density in the layers above the surface is lowest for the diblock geometry, as may be seen in the plot in Figure 2. Since the B tails are the longest for this structure, as noted above, the layer thickness is greatest and, thus, the polymer density extends furthest in this curve.

The general features of the triblock are more similar to the diblock than the other chains examined in this sample. Here, however, two short B tails extend from either side of the adsorbed chain. Consequently, these molecules contribute to a higher segment density in the layers immediately above the wall than do the single, sparsely spaced B tails in the diblock structure. Since the tails are not as long as those in the diblock, the polymer film produced from the triblock is thinner than that formed from the diblock chains. The triblock architecture will be discussed in further detail in the subsequent section.

The surface coverage is not only a function of the fraction of A's and B's in contact with the surface but also the number of chains that bind to this wall. As can be seen in Table Ia (and Figure 2), the number of bound chains, and consequently the surface coverage, increases as $\langle n_A \rangle$ decreases. This phenomenon can again be understood from the 2D figures and the preceding discussion. In particular, we noted that the alternating copolymers bind to the surface in long loops and tails. The chains effectively occupy a smaller area on the surface than the case of the blocky copolymers, which, due to the longer rows of contiguous stickers, stretch out along the surface. Thus, there are more vacant surface sites for new, incoming chains to occupy in the case of the alternating architecture. Consequently, we observe a higher number of bound chains and, thus, a higher surface coverage for this type of copolymer (see Table Ia).

It is worth further noting that the number of bound chains is higher for the diblock than the triblock architecture. This data indicates that a B tail at both ends of the chain is more effective at sterically hindering chains from approaching the surface than a B block that is twice as long but located at only one end of the chain.

Having contrasted the extremes, alternating and blocky, we now turn to an intermediate or random sequence distribution. Figure 3b shows the surface adsorption of random chains in two dimensions. As Table I indicates the fraction of bound A's is comparable for the random and alternating copolymers but a higher fraction of A's bind for the blocky chains. Since the run length, $\langle n_A \rangle$, for the random copolymer is not sufficiently long that each chain is stretched out along the surface, a slightly higher number of chains bind to the surface for the random case than the blocky one.

Upon analysis of the behavior of the B units, it is important to recall that the random chain also contains some short alternating (ABA) runs. If both such A's bind, they drag the interconnecting B to the surface. Thus, the fraction of bound B's is higher here than in the case of the blocky chains (where no ABA runs are present) but is lower than the value obtained from the purely alternating copolymers.

The results in this section show qualitative agreement with recent self-consistent-field calculations performed by van Lent on the surface adsorption of AB block and random copolymers, where the A's are attracted to the surface and the B's are compatible with the B solvent.[9] In particular, van Lent finds that, for a fixed concentration of the A's in a chain, the fraction of A's bound at the interface increases with block length, as is also apparent from our values in Table Ia. With increasing block length, the A's can form longer trains of stickers along the surface. Consequently, his calculations for diblocks also reveal a dense layer of A's at the interface, with the B's dangling into the solution.

Having analyzed chains where the ratio of A to B molecules was held fixed, we now turn our attention to various BAB and ABA type copolymers in which we systematically vary the ratio of these two types of molecules. From these studies, we gain further insight into the adsorption behavior of triblock copolymers and other chains for which these segments are representative of the entire copolymer sequence distribution.

BAB Triblocks. As a test of our simulations, we initially examined the irreversible adsorption ($P = 0$) of BAB triblocks, where the length of the central A block was held constant at 3 lattice sites. The length of both B arms was identical and systematically varied from 5–20 lattice sites. Since the chains bind irreversibly, there is no possibility for the kind of structural rearrangement that would improve the packing density of the chains at the surface. Thus, the concentration of chains at the surface was fairly dilute, and each B arm behaves as an unperturbed self-avoiding random-walk in three dimensions. Consequently, the extension of the chain in the Z direction, or D, should scale like $N^{3/5}$, where N is the arm length.[20] Since the A segments are so short, the surface coverage will be dominated by the properties of the weakly adsorbing B moieties. In particular, the fraction of bound molecules, f_b (the surface coverage), should scale with $1/D$, as in the case of adsorbed homopolymers.[21] To test whether the results of our simulation coincide with this prediction, we plotted the natural logarithm of the surface coverage versus the natural logarithm of the B arm length. The resulting line has a slope of -0.59 ± 0.03, which shows that the predicted scaling relationship between f_b and D is satisfied. This test gives credence to future predictions from the model, which are most important in the cases where such simple scaling laws may not apply.

The next examples we will consider are also BAB triblocks; however, here the length of the whole chain is held constant at 33 lattice sites, while both $\langle n_A \rangle$ and $\langle n_B \rangle$ are varied. Figure 4 shows the SDD for various BAB triblock copolymers, and Figure 5 shows the graphical output from a 2D simulation. Here, $\langle n_A \rangle$ varies from 3 to 11 units, while $\langle n_B \rangle$ varies from 15 to 11 lattice sites. As can be seen, the surface coverage increases as the ratio $\langle n_A \rangle / \langle n_B \rangle$ increases. A roughly 6-fold increase in $\langle n_A \rangle$ yields only an approximately 3-fold increase in the surface coverage. Coverage of the surface layer is provided by both A and B molecules. Even though the actual number of A's attached to the surface increases as $\langle n_A \rangle$ is increased, the number of B molecules located at the interface decreases. Consequently, the surface coverage does not scale linearly with the length of the A block.

Table IIa, which lists the fraction of bound A's and B's and the total number of chains, provides further insight into the adsorption behavior of these chains. In particular, note that, as $\langle n_A \rangle$, increases, *the fraction* of bound A's decreases, while the number of bound chains increases. As $\langle n_A \rangle$ increases, it becomes more difficult to accommodate the long run of A's directly on the surface. However, an increase in $\langle n_A \rangle$ results in a decrease of the arm length $\langle n_B \rangle$. This, in turn, results in an increase in the total

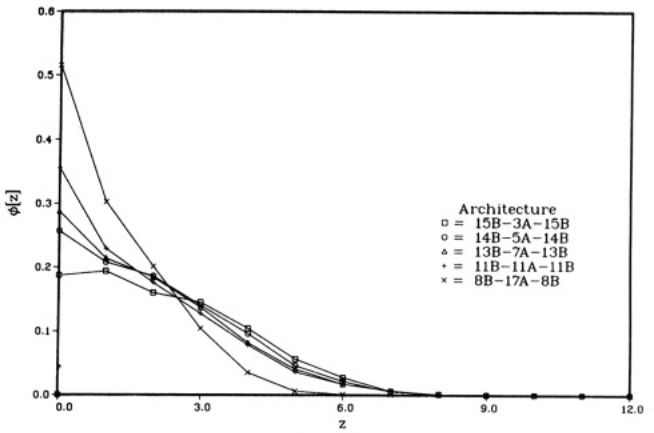

Figure 4. SDD's for the various BAB triblocks. The numbers next to the letters indicate the number of molecules of that particular type that exist in the chain. Only the adsorbed chains are included in the calculation of the SDD. (Each plot represents values from a single run of the relevant simulation, while the values of surface coverage in the tables are obtained from averaging two independent simulation runs.)

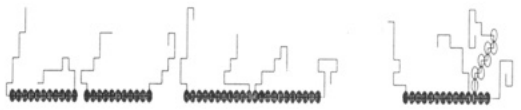

Figure 5. Graphical output from the simulations in two dimensions for BAB copolymers. Here $\langle n_A \rangle = 11$ and $\langle n_B \rangle = 11$.

number of bound chains, since there is less of the B block to sterically hinder new chains from approaching and binding to the surface.

Note that the layer thickness, or extension of the film in the Z direction, also decreases as $\langle n_B \rangle$ is decreased. Thus, it is the stretching of the B segments into the solution that is primarily responsible for the height of the polymer film.

Other distinctive features of the adlayer can be noted from the graph in Figure 4. As can be clearly seen for the cases where $\langle n_A \rangle = 5$ and 7, there exists a local minimum in the curve a few layers away from the surface. This phenomenon can best be understood by referring to the 2D picture in Figure 5. The majority of the A units lie at the surface (see Table IIa), giving rise to the high polymer density in this plane. A few layers away, there is a dearth of A's and the B units lie stretched away from the interface. In this region, each B arm intersects a particular plane only once. Thus, the segment density in these planes is relatively low. Further away from the surface, the B molecules do not feel the presence of the wall; thus, the molecules curl back on themselves in the manner of self-avoiding chains. Consequently, the chain may intersect a particular plane more than once. This phenomenon causes the subsequent rise in the SDD after the initial drop in the polymer density. As $\langle n_A \rangle$ increases, a larger surface area is covered by each A block. Hence, the average separation between B segments extending away from the adsorbed A blocks increases and the local B concentration in the $Z = 2$ and 3 planes decreases.

When the chain is composed almost entirely of B segments, the polymer density at the surface is actually at a minimum (see Figure 4). Since the B's are not attracted to the wall, the highest concentration of polymer is found a few layers away from this interface.

$B_{13}A_7B_{13}$ versus $A_3B_{27}A_3$. In order to develop a further appreciation for the affect of molecular architecture on adsorption, we examine a chain that is still 33 lattice sites in length but now the geometry is that of an ABA triblock. In particular, we let $\langle n_A \rangle = 3$ blocks and $\langle n_B \rangle = 27$. By comparing the behavior of this polymer with the BAB case where $\langle n_A \rangle = 7$ and $\langle n_B \rangle = 26$, we can observe differences in properties that arise simply from taking two $\langle n_A \rangle \sim 3$ blocks and placing them both at the center versus putting one on each end.

The most significant difference between the two cases arises in the number of chains that are bound to the surface. At equilibrium, there are 73.5 bound chains for the BAB geometry (averaged over two runs), while for the ABA chains, there are 105 polymers on the surface. The difference in the number of bound molecules gives rise to the observed differences in the SDD curves (Figure 6). Since more ABA molecules bind, the SDD (the number of polymer segments in a given Z plane) is consistently higher in thise case than for the BAB molecules. As noted above, in the BAB case, a high fraction of the A's (92%) are bound on the surface. This implies that the $\langle n_A \rangle$ monomers are stretched out along the wall. (Here, the loss in entropy is outweighed by the gain in energy, since the A–surface interaction is highly attractive. Thus, there is little driving force for the chains to desorb and reattach with fewer stickers at the interface.) Consequently, each adsorbed polymer occupies a significant surface area, leaving less available space for new, incoming molecules. Furthermore, the long solvent-compatible B arms stretch away from the interface and sterically hinder new chains from binding to the wall. Both effects (the energetically favorable stretching of the A's along the wall and of the B's into the solution) contribute to the low number of chains at the surface.

In the initial stages of ABA adsorption, the majority of the chains bind with both A units on the surface. As the surface becomes crowded, the chains must bind in narrow hairpin loop conformations, which occupy less surface area. This structure, though entropically unfavorable, is nonetheless energetically favored since it maintains the high number of A–surface contacts. At even higher surface coverage, only one end of the ABA chain can access the surface and the remainder of the chain forms a tail that extends into solution. (This explains why the fraction of bound A's in Table II is less for $A_3B_{27}A_3$ than $B_{13}A_7B_{13}$.) Thus, more ABA chains can pack onto the surface than BAB copolymers of comparable composition.

Figure 7 shows the SDD curves for all the cases examined in which N, the chain length, is equal to 33 lattices sites. The most significant difference between the various cases is the great variation in surface coverage that arises from the different polymer geometries. By placing all the curves in one graph, we can see that the values for surface coverage are more sensitive to the actual number of A units in the chain than differences in sequence distribution for a fixed number of A's. However, the variations in polymer density decrease in subsequent layers, and the height of the polymer film is essentially comparable for all the architectures. Thus, while surface coverage is sensitive to $\langle n_A \rangle$, the film thickness is primarily determined by N, the degree of polymerization.

ABA Triblocks. In order to keep the size of the B loop sufficiently large while simultaneously varying the length of $\langle n_A \rangle$, we increased the entire length of the ABA polymers to 50 lattice sites. This chain length was held constant, while the ratio of $\langle n_A \rangle$ to $\langle n_B \rangle$ was varied. Figure 8 shows the SDD for the various chains examined, and Figure 9 shows the graphical output from the 2D calculation. Here too, the surface coverage increases as $\langle n_A \rangle$ is increased. The peaks in the density curves that occur away from the wall are attributable to segments of the large B loops that

Table II

polymer	f_A,[a] %	f_B,[b] %	no. of bound chains	surface coverage,[c] %	ave layer thickness[d]
			(a)		
$B_{15}A_3B_{15}$	99.9 ± 0.3	13.6 ± 0.5	67 ± 2.8	19.6 ± 0.2	7.12 ± 0.16
$B_{14}A_5B_{14}$	97.2 ± 0.2	13.9 ± 0.4	73 ± 1.4	27.5 ± 2.0	6.69 ± 0.04
$B_{13}A_7B_{13}$	91.9 ± 1.3	12.4 ± 0.4	73.5 ± 2.1	29.9 ± 0.9	6.67 ± 0.04
$B_{11}A_{11}B_{11}$	87.7 ± 0.9	12.7 ± 0.2	79 ± 4.2	39.3 ± 3.3	6.19 ± 0.35
$B_8A_{17}B_8$	73.5 ± 1.1	12.9 ± 0.2	88.5 ± 3.5	53.7 ± 2.4	5.36 ± 0.18
$A_3B_{27}A_3$	79.6 ± 1.5	11.0 ± 0.2	105 ± 2.1	34.1 ± 1.6	6.40 ± 0.07
			(b)		
$B_{15}A_3B_{15}$	100 ± 0.0	5.7 ± 0.5	62.5 ± 4.6	12.2 ± 0.6	7.29 ± 0.14
$B_{14}A_5B_{14}$	97.7 ± 1.2	5.8 ± 0.1	69 ± 1.4	18.7 ± 0.1	7.07 ± 0.22
$B_{13}A_7B_{13}$	94.8 ± 0.9	4.8 ± 0.5	72.5 ± 0.7	23.8 ± 0.4	7.00 ± 0.11
$B_{11}A_{11}B_{11}$	86.6 ± 0.6	5.8 ± 0.5	81 ± 1.4	36.5 ± 1.3	6.55 ± 0.08

[a] Percent of A molecules bound to the surface. [b] Percent of B molecules bound to the surface. [c] Percent of sites at $Z = 0$ covered by polymer sites (either A or B). [d] This quantity is the maximum Z coordinate for each bound chain, averaged over all the absorbed chains.

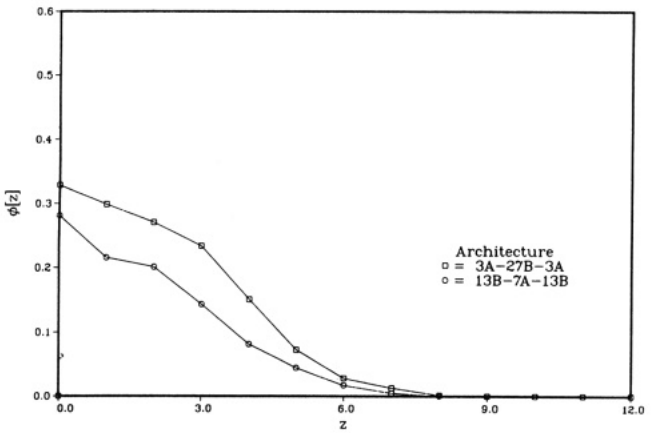

Figure 6. SDD's for the $B_{13}A_7B_{13}$ and $A_3B_{27}A_3$ triblocks.

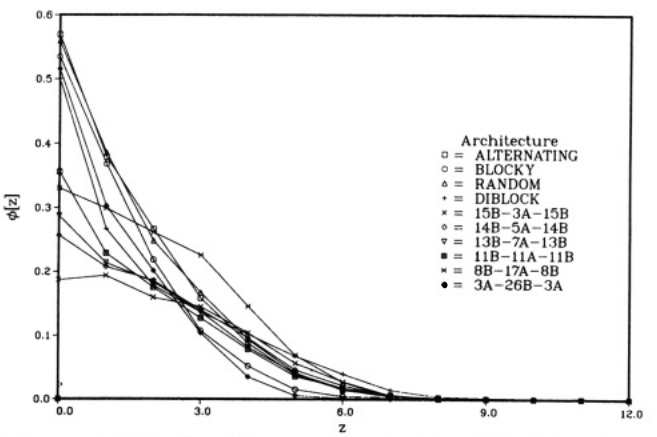

Figure 7. SDD's for all the cases examined in which N, the chain length, is equal to 33 lattice sites. Only the adsorbed chains are included in the calculation of the SDD. (Each plot represents values from a single run of the relevant simulation, while the values of surface coverage in the tables are obtained from averaging two independent simulation runs.)

behave as self-avoiding walks in the solution.

Table III shows the fraction of bound A's and B's and the total number of chains attached to the wall. Note that, despite the large variations in $\langle n_A \rangle$ and $\langle n_B \rangle$, the number of chains bound at the interface remains essentially constant. This is a consequence of two factors. In the case where $\langle n_A \rangle \ll \langle n_B \rangle$, it is the large, intervening B loops that sterically hinder chains from the surface. In the cases where $\langle n_A \rangle \sim \langle n_B \rangle$ and $\langle n_A \rangle$ is large, it is the significant surface area occupied by the A's, and subsequently the entire polymer, that prohibits new chains from adsorbing to the wall (see Figure 9).

Another important point is the significant decrease in the fraction of bound A's as $\langle n_A \rangle$ increases. For the first

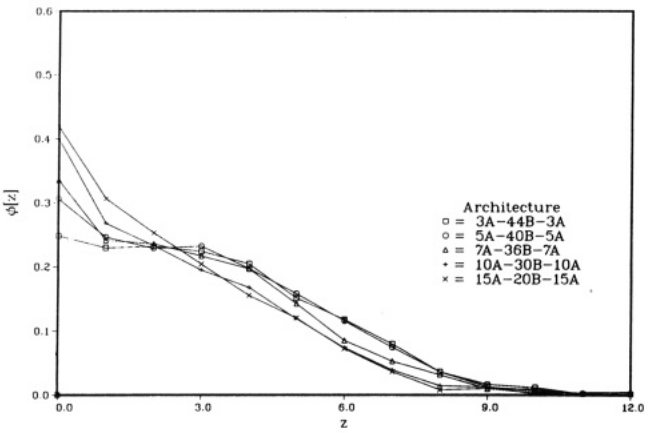

Figure 8. SDD's for the various ABA triblocks. The numbers next to the letters indicate the number of molecules of that particular type that exist in the chain. Only the adsorbed chains are included in the calculation of the SDD. (Each plot represents values from a single run of the relevant simulation, while the values of surface coverage in the tables are obtained from averaging two independent simulation runs.)

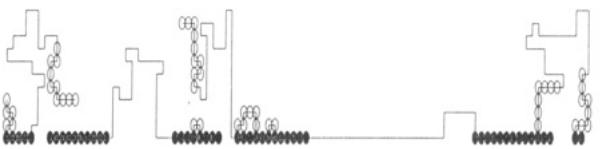

Figure 9. Graphical output from the simulations in two dimensions for ABA copolymers. Here $\langle n_A \rangle = 10$ and $\langle n_B \rangle = 30$.

set of chains that bind to the surface, the $\langle n_A \rangle$ stickers form long trains along the wall. These structures prevent later segments from interacting fully with the surface and thereby cause subsequent chains to form tail and loop configurations. (Note that, though the fraction of bound A's decreases as $\langle n_A \rangle$ increases, the *actual number* of bound A's is greater if $\langle n_A \rangle$ is increased and the number of bound chains remains constant (see eq 2). Thus surface coverage, which depends on the number of bound A's (and B's), also increases as $\langle n_A \rangle$ gets bigger.)

Contrary to the dramatic change in the fraction of bound A's, the fraction of bound B's remains relatively constant for the different $\langle n_B \rangle$'s examined. Thus, for sufficiently long runs of B molecules, the run length forms a loop that stretches away from the surface. Increasing the size of the loop does not significantly increase the number of B molecules at the surface; it just enhances the polymer density in outer layers of the polymer film and increases the overall thickness of the adlayer (see last column in Table IIIa).

Table III

polymer	f_A,[a] %	f_B,[b] %	no. of bound chains	surface coverage,[c] %	ave layer thickness[d]
			(a)		
$A_3B_{44}A_3$	80.9 ± 0.8	7.5 ± 0.3	80 ± 2.8	27.2 ± 1.8	8.40 ± 0.15
$A_5B_{40}A_5$	66.4 ± 1.4	7.0 ± 0.2	81 ± 4.2	32.1 ± 0.4	8.12 ± 0.22
$A_7B_{36}A_7$	60.4 ± 0.8	7.0 ± 0.4	78 ± 1.4	35.4 ± 0.7	7.90 ± 0.21
$A_{10}B_{30}A_{10}$	54.1 ± 0.6	7.1 ± 0.3	80 ± 2.8	43.1 ± 1.5	7.73 ± 0.12
$A_{15}B_{20}A_{15}$	41.8 ± 1.2	6.4 ± 0.2	81 ± 3.5	46.1 ± 1.9	7.41 ± 0.12
			(b)		
$A_3B_{44}A_3$	78.4 ± 3.7	2.6 ± 0.1	69 ± 2.8	16.7 ± 0.6	8.59 ± 0.06
$A_5B_{40}A_5$	71.2 ± 0.8	3.2 ± 0.7	72.5 ± 1.4	25.4 ± 0.8	8.55 ± 0.33
$A_7B_{36}A_7$	63.5 ± 2.8	2.0 ± 0.1	77 ± 1.4	30.9 ± 1.2	8.22 ± 0.11
$A_{10}B_{30}A_{10}$	53.4 ± 1.0	1.9 ± 0.2	79 ± 1.4	37.0 ± 0.9	8.00 ± 0.01
$A_{15}B_{20}A_{15}$	41.3 ± 0.6	1.9 ± 0.1	75.5 ± 1.4	40.2 ± 0.2	7.63 ± 0.07

[a] Percent of A molecules bound to the surface. [b] Percent of B molecules bound to the surface. [c] Percent of sites at $Z = 0$ covered by polymer sites (either A or B). [d] This quantity is the maximum Z coordinate for each bound chain, averaged over all the adsorbed chains.

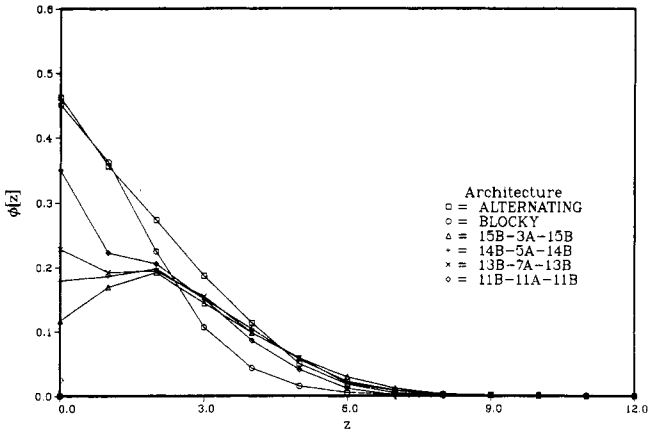

Figure 10. SDD's where $\chi_{BS} = 1$ for chains of length 33. Only the adsorbed chains are included in the calculation of the SDD. (Each plot represents values from a single run of the relevant simulation, while the values of surface coverage in the tables are obtained from averaging two independent simulation runs.)

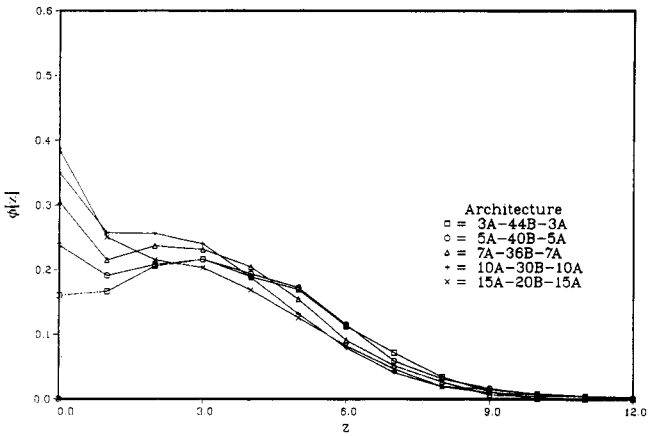

Figure 11. SDD's where $\chi_{BS} = 1$ for chains of length 50. Only the adsorbed chains are included in the calculation of the SDD. (Each plot represents values from a single run of the relevant simulation, while the values of surface coverage in the tables are obtained from averaging two independent simulation runs.)

$\chi_{BS} = 1.0$. In the final computer experiment for the adsorption of AB copolymers onto a solid surface, we weighted the probability that the chains will bind to the surface by a factor $q = \exp(-n_B\chi_{AB})$ and set χ_{AB} equal to 1.0. We then recalculated the SDD for various architectures examined in the previous investigations (see Figures 10 and 11). Part b of Tables I–III shows the recalculated values of the various parameters when $\chi_{BS} = 1.0$ for the respective systems. The most dramatic effect common to all these cases was to lower the total surface coverage. The cases most affected were the alternating and blocky copolymers, where $\langle n_A \rangle$ is relatively small. In these situations, there is a high concentration of A's that are in close proximity to B molecules. Thus, increasing the B–surface repulsion causes a few neighboring A's to be dragged away from the interface along with the repelled B's. The repulsion of the B's away from the surface also enhances the height of the polymer film in several of the cases examined here. This later phenomenon has also been observed by Aquilera-Granja and Kikuchi through their computer model for the adsorption of random copolymers.[5]

In terms of the overall shape of the BAB SDD curves, the case in which the chain is composed primarily of B's ($\langle n_A \rangle = 3$ and $\langle n_B \rangle = 15$) showed the most significant change. With $\chi_{AB} = 1.0$, the polymer density at the surface is substantially reduced. The strong repulsion has forced the majority of the species on the bound chains from the surface and into the subsequent layers of the film.

The trend is also seen in the ABA chains: the chains with the fewest A's and, thus, largest number of B's are most affected by enhancing the B–surface repulsion. What is remarkable is the extent to which the polymer densities in the second and third layers are also reduced from their original values. Thus, the repulsive nature of the surface is transmitted to layers that are one or two lattice sites away. In essence, biasing specific segments away from the surface also influences the location of the contiguous or neighboring segments.

Conclusions

From the above calculations, it is clear that the structure of an adsorbed copolymer film is influenced not only by the fraction of stickers in the chain but also by the arrangement of these stickers along the chain. For chains having a fixed composition, subtle but real differences are seen between the alternating, random, and blocky architectures. The diblock and BAB triblock structures provide the highest fraction of A's that are adsorbed at the interface. Consequently, these later structures will provide a greater adhesion between the copolymer and the substrate. Furthermore, from Table Ia, it is clear that it takes fewer triblock chains than the other sequence distributions to provide a comparable surface coverage. Thus, we can say that the efficiency of the adsorption process is highest for this structure.

We conclude by comparing the general features that characterize a chain that terminates in an A block with the characteristics of a chain that is capped by a length of B molecules. Insight into the effect of adding a short A block at the end of an AB copolymer may be obtained by comparing the results for the $A_3B_{27}A_3$ and $B_{13}A_7B_{13}$ chains. In particular, this sticky terminal block contributes

to (1) an increase in the number of bound chains at the interface, since the surface interaction is highly attractive, (2) an increase in the surface coverage, and (3) a decrease in the film thickness, since the sticky end will pull neighboring B segments from the solution down onto the surface.

On the other hand, capping a chain with a longer A block will result in a different set of characteristics. The effect of a longer A block at the end of a copolymer may be assessed by comparig the results from chains $A_{10}B_{30}A_{10}$ and $A_3B_{27}A_3$ chains. In particular, this long block contributes to (1) a decrease in the number of bound chains since the long $\langle n_A \rangle$ fragments that are bound directly to the surface decrease the area available for new chains, (2) an increase in surface coverage (given that the effect from number (1) is not too drastic), since the actual number of A's that can interact with the surface has been increased, and (3) an increase in the layer thickness, since the long A fragments cannot all bind directly onto the surface. Thus, some chains bind with only a few stickers at the interface, and the remainder of the chain forms a tail that extends into the solution. (This increase in layer thickness will also result from the increase in the molecular weight of the chain, which arises from the addition of the long A block.)

The presence of a B block, whether short or long, at the end of a chain contributes to (1) a decrease in the surface coverage since the segment sterically hinders polymers from adsorbing onto the interface and (2) an increase in the film thickness.

We hope the results presented in this report will encourage further experimental investigations into the effect of molecular architecture on the surface adsorption of copolymer chains in solution.

Acknowledgment. A.C.B. gratefully acknowledges financial support from the National Science Foundation, through Grant DMR-8718899, and PPG Industries. C.W.L. thanks B. van Lent for stimulating discussions and the copy of his thesis.

References and Notes

(1) For a review of the literature, see: (a) Cohen Stuart, M. A.; Cosgrove, T.; Vincent, B. *Adv. Colloid Interface Sci.* **1986**, *24*, 143. (b) Fleer, G. J.; Scheutjens, J. M. H. M.; Cohen, Stuart, M. A. *Colloids Surf.* **1988** *31*, 1. (c) de Gennes, P.-G. *Adv. Colloid Interface Sci.* **1987**, *27*, 189. (d) Kawaguchi, M.; Takahashi, A. *Adv. Polym. Sci.* **1982**, *46*, 1.
(2) Marques, C.; Joanny, J. F.; Leibler, L. *Macromolecules* **1988**, *21*, 1051 and references therein.
(3) Balazs, A. C.; Lewandowski, S. *Macromolecules* **1990**, *23*, 839.
(4) Cosgrove, T.; Crowley, T. L.; Mallagh, L. M.; Ryan, K.; Webster, J. R. P. *Polym. Prepr. (Am. Chem. Soc., Div. Polym. Sci.)* **1989**, *31*, 370.
(5) Aquilera-Granja, F.; Kikuchi, R. *Lectures on Thermodynamics and Statistical Mechanics*; Lopex de Haro, M., Varea, C., Medina-Noyola, M., Eds.; World Scientific: Teaneck, N. J., to be published.
(6) For the behavior of *bulk* triblock, diblock, and random copolymers at an interface, see: Theodorou, D. N. *Macromolecules* **1988**, *21*, 1422.
(7) Marques, C. M.; Joanny, J. F. *Macromolecules* **1990**, *23*, 268.
(8) Garel, T.; Huse, D. A.; Leibler, S.; Orland, H. *Europhys. Lett.* **1989**, *8*, 9.
(9) (a) van Lent, B. Molecules Structure and Interfacial Behavior of Polymers. Ph.D. Thesis, Agricultural University, Wageningen, The Netherlands, 1989. (b) van Lent, B.; Scheutjens, J. M. H. M. *Macromolecules* **1989**, *22*, 1931.
(10) Balazs, A. C.; Huang, K.; Lantman, C. W. *Macromolecules* **1990**, *23*, 4641.
(11) (a) Hone, D.; Hong, J.; Pincus, P. *Macromolecules* **1987**, *20*, 2543. (b) Hong, J.; Hone, D. *Macromolecules* **1988**, *21*, 2600.
(12) Douglas, J. F. *Macromolecules* **1989**, *22*, 3707.
(13) Svrakic, N. M.; Privman, V. *Lecture Notes in Physics, Vol. 338: Directed Models of Polymers, Interfaces, and Clusters: Scaling and Finite-Size Particles*; Springer-Verlag: Berlin, 1990; p 61.
(14) Balazs, A. C.; Siemasko, C. P.; Lantman, C. W., *J. Chem. Phys.*, in press.
(15) Verdier, P. H.; Stockmayer, W. H. *J. Chem. Phys.* **1962**, *36*, 227.
(16) Hilhorst, J. H.; Deutch, J. M. *J. Chem. Phys.* **1975**, *63*, 5153.
(17) Kolb, M. *J. Phys. A* **1986**, *19*, L263.
(18) Cosgrove, T.; Heath, T.; van Lent, V.; Leermakers, F.; Scheutjens, J. *Macromolecules* **1987**, *20*, 1962.
(19) Balazs, A. C.; DeMeuse, M. T. *Macromolecules* **1989**, *22*, 4260.
(20) Flory, P. J. *Principles of Polymer Chemistry*; Cornell University Press: Ithaca, NY, 1953.
(21) de Gennes, P.-G. *Scaling Concepts in Polymer Physics*; Cornell University Press: Ithaca, NY, 1979, p 35.